*Pramana – J. Phys.* (2019) 92:30
https://doi.org/10.1007/s12043-018-1703-1



# Design of optical Mach–Zehnder interferometer phase shifter in silicon-on-insulator

NAGARAJU PENDAM* and C P VARDHANI

Department of Physics, Osmania University, Hyderabad 500 007, India
*Corresponding author. E-mail: pnrphysics84@osmania.ac.in

MS received 30 May 2017; revised 5 August 2018; accepted 8 August 2018; published online 1 February 2019

**Abstract.** A passive TE mode phase shifter-based compact structure of optical Mach–Zehnder interferometer (MZI) using silicon-on-insulator (SOI) platform is demonstrated by using BPM simulations. Insertion loss was found, that is 9 dB for 3 $\mu$m width, 16 dB for 1.55 $\mu$m wavelength, 0.9 dB for 2000 $\mu$m path length (arms), and 15 dB for 0.0055 index differences between the core and the cladding of SOI of the designed device. The Mach–Zehnder interferometer attains good phase shifts by changing the path lengths (arm) with TE mode polarisation.

**Keywords.** Mach–Zehnder interferometer; insertion loss; optical phase shifter; simulation software; silicon-on-insulator.

**PACS Nos 42.81.Dp; 42.82.−m; 42.82.Et; 42.79.Pw**

## 1. Introduction

Silicon-based devices are frequently used in microfabrication industry now a days. The potential of these devices helps in monolithic integration of optical and electronic devices developed in silicon-on-insulator substrate. The silicon-on-insulator (SOI) Mach–Zehnder interferometers (MZI) are optically transparent at long-haul communication wavelengths, high speed optical modulator [1], polarisation beam splitter [2], integrated p–n junction [3], refractive index dependence sensor [4], quantum photonic circuits [5], photonic crystal fibre [6], low power carrier depletion modulator [7,8], monolithic fabrication [9,10], phase shifter [11], Mach–Zehnder-based directional coupler [12], polarisation division multiplexed quadrature phase shift keying [13], TE mode polarisation splitter [14], slot waveguides [15], optical biosensor [16–18], photonic signal processor cores [19], Pound–Drever–Hall laser stabilisation system to reduce the noise of stable lasers [20], broadband directional coupler switch [21,22], band transmitters from photonic to electronic devices [23] flexible photonic devices for biophotonic probes [24], protein detection [25], MZI coupler resonant waveguide optical gyroscopes [26], dual output MZI for noise cancellation [27], pulse generation [28] and tunable plasmonic filter with ring resonators [29]. SOI substrate has possessed high index contrast, easy-to-fabricate rib structured devices, strongly confined optical mode, exhibits low losses, easy-to-get total internal reflection for guiding the field, high integration density, compatible with Si electronics, low-cost compared to other InGaAsP/InP or $LiNbO_3$ substrates. This MZI configuration is completely novel on SOI substrate for obtaining phase shifts and low insertion losses using S-bend and straight waveguides with one output and one input compared to $LiNbO_3$, InP, silver ion exchange on glass material and plasmonic substrates.

In this paper, we discuss the variation of symmetrical MZI, intensity, phase shifts, and insertion losses with TE polarisation-dependent mode which is the dominant mode in optical communication compared to the TM mode. This device also examined coupling parameters such as width, wavelength, index difference and coupling length (length of the middle S-bend waveguides). In this article, we propose a design of MZI on SOI platform by using an R-Soft CAD tool and simulated through beam propagation method (BPM) at 1550 nm wavelength. The outcomes are reported based on simulation results because of the lack of fabrication facility and the main purpose is to obtain the best optimised device for further fabrication.

## 2. Device structure

The schematic diagram of the proposed MZI is shown in figure 1. It consists of two waveguides which are

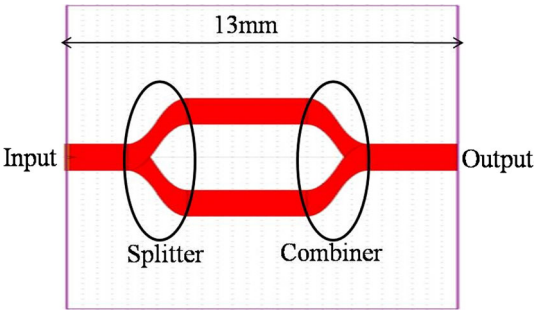


**Figure 1.** Schematic diagram of MZI.

straight and S-bend waveguides on SOI substrate with slab structure. MZI comprises two back-to-back power splitters connected by a pair of widely separated straight waveguides. In the MZI, the guided light is divided into two beams and it propagates through two straight waveguides (arms), combined by a splitter and comes out through the straight waveguide. Total length of the MZI is 13 mm, input power is 1 $\mu$W, width is 5 $\mu$m, height is 5 $\mu$m, input straight waveguide is 2 mm, S-bend waveguide is 2 mm, separated waveguide is 4 mm and output straight waveguide is 3 mm, separation between two straight waveguides is 18 $\mu$m, index difference is 0.0067 (0.3% of core Si and cladding $SiO_2$) within the SOI regions.

## 3. Simulation results

The BPM is the most powerful method to investigate linear and nonlinear light-wave propagation phenomena in axially varying waveguides. The BPM is the most widely used propagation technique for modelling integrated and fibre optic photonic devices. The BPM is essentially a particular approach for approximating the exact wave equation for monochromatic waves and solving the resulting equations numerically. The basic approach is illustrated by formulating the problem under the restrictions of a scalar field (i.e. neglecting polarisation effects) and paraxiality (i.e. propagation restricted to a narrow range of angles). The scalar field assumption allows the wave equation to be written in the form of the well-known Helmholtz equation for monochromatic waves.

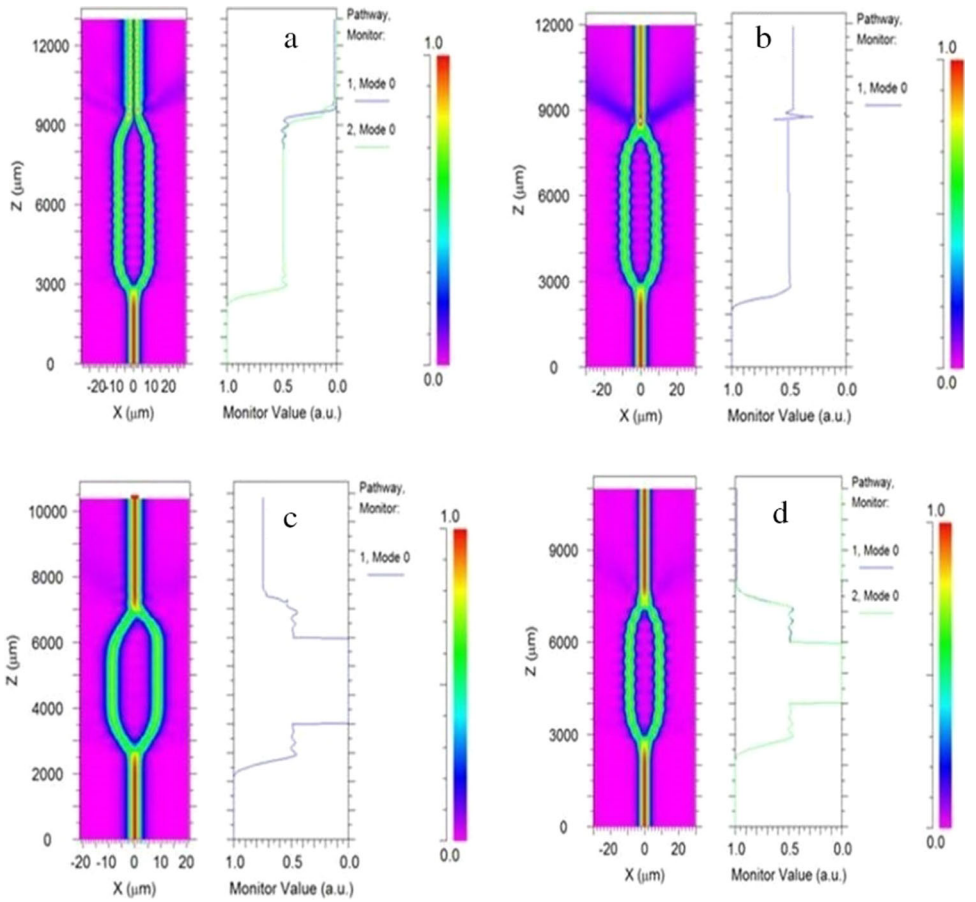


**Figure 2.** Simulated optical power distribution profiles for MZI mode propagations: (**a**) 180° phase shift, (**b**) 90° phase shift, (**c**) 45° phase shift and (**d**) 0° phase shift.

$$\frac{\partial^2\Phi}{\partial x^2}+\frac{\partial^2\Phi}{\partial y^2}+\frac{\partial^2\Phi}{\partial z^2}+k(x,y,z)^2\,\Phi=0. \quad (1)$$

Here the scalar electric field is written as $E(x, y, z, t) = \Phi(x, y, z)\,\mathrm{e}^{-\mathrm{i}wt}$ and the notation $k(x, y, z, t) = k_0 n(x, y, z)$ is introduced for the spatially-dependent wave number, with $k_0 = 2\pi/\lambda$ being the wave number in free space. The geometry of the problem is defined entirely by the refractive index distribution $n(x, y, z)$. Assuming that axis is predominantly along the $z$-direction, it is beneficial to factor the rapid phase variation out of the problem by introducing the so-called slowly varying field $u$ along the direction $z$

$$\Phi(x, y, z) = u(x, y, z)\,\mathrm{e}^{\mathrm{i}k_z}. \quad (2)$$

$\bar{k}$ is a constant chosen to represent the average phase variation of the field $\Phi$. Then, introducing the expression into the Helmholtz equation yields the following equation for the slowly varying field:

$$\frac{\partial^2 u}{\partial z^2}+2\mathrm{i}\bar{k}\frac{\partial u}{\partial z}+\frac{\partial^2 u}{\partial x^2}+\frac{\partial^2 u}{\partial y^2}+(k^2-\bar{k}^2)u=0. \quad (3)$$

$$\frac{\partial u}{\partial z}=\frac{\mathrm{i}}{2\bar{k}}\left(\frac{\partial^2 u}{\partial x^2}+\frac{\partial^2 u}{\partial y^2}+(k^2-\bar{k}^2)u\right). \quad (4)$$

Equation (3) is the basic BPM equation in three dimensions (3D) and simplification to two dimensions (2D) is obtained by omitting any dependence on $y$ [30].

Simulations have been carried out by the BPM tool to identify the propagation of an optical signal of the fundamental TE polarisation mode through the MZI. We depicted some of the simulation profiles in figures 2 and 3. Figure 2a shows the top view of the optical power distribution for MZI mode propagation with 180° phase shift at 4000 $\mu$m path length. Figure 2b shows the top view of the optical power distribution for MZI mode propagation with 90° phase shift at 3000 $\mu$m path length. Figure 2c shows the top view of the optical power distribution for MZI mode propagation with 45° phase shift at 2000 $\mu$m path length. Figure 2d shows the top view of the optical power distribution for MZI mode propagation with 0° phase shift at 1000 $\mu$m path length. Figure 3a shows the 3D view of simulation of MZI at 5 $\mu$m width, 1550 nm wavelength, 13 mm length, 4000 $\mu$m coupling length and 18 $\mu$m gap between the two separated waveguide arms. Figure 3b shows the amplitude view of MZI, and from this profile it can be seen that phase shift is equally divided to half of its maximum propagating wave. According to the interferometer theory, the change of intensity is due to the phase of the wave which is directly related to the change of length between the two splitters (path length), wavelength, refractive index difference and width of the waveguide.

## 4. Results and discussion

Figure 4 shows the variation of phase shifts and intensity with MZI parameter path length, which is the length between two splitters of the MZI. It reports that the phase shift is directly proportional to the path length and intensity is directly proportional to the path length. We optimised 4000 $\mu$m path length because it gives maximum value of intensity and phase shift.

The coupling parameter width ($w$) of the device influences the transmitted power as well as the insertion loss. Figure 5 shows that the transmitted power and insertion loss vary with component width of the MZI in TE polarisation mode (dominant mode in optical communication range). The transmitted power decreases with width, because the effective index is less sensitive to width, which has got a lesser transmitted power of 0.1 $\mu$W at 3 $\mu$m width. A maximum transmitted power of 0.003 $\mu$W is obtained at 8 $\mu$m width as higher widths enable optimal mode confinement of the light inside the device. The insertion loss is reciprocal to the transmitted power and hence

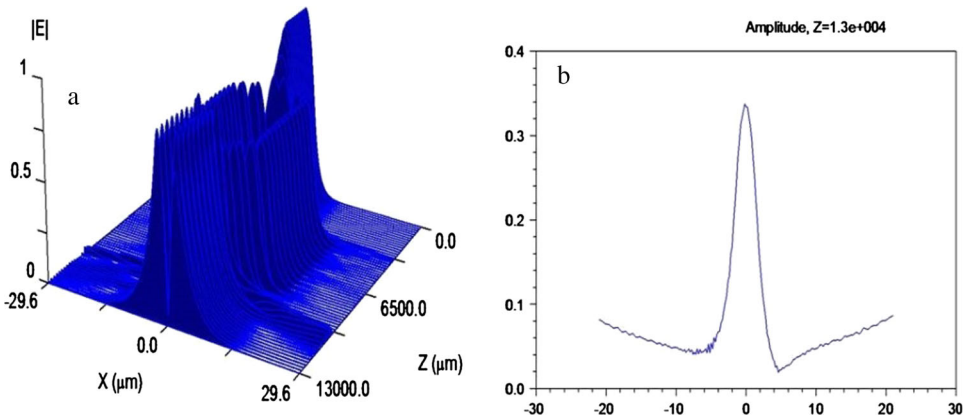


**Figure 3.** Simulation profiles of MZI at 4000 $\mu$m path length: **(a)** 3D view and (**b**) amplitude view.

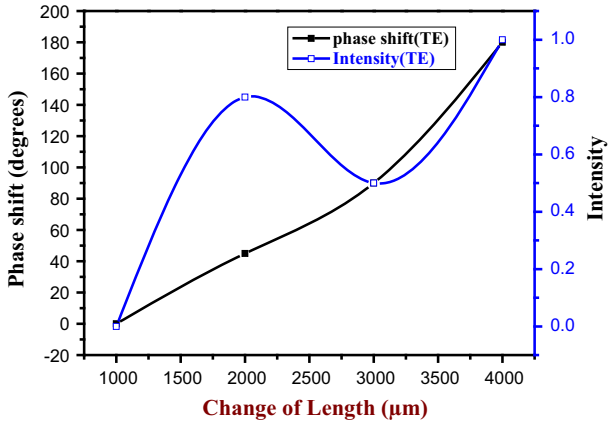


**Figure 4.** Plots between phase shift and intensity vs. path lengths between two splitters.

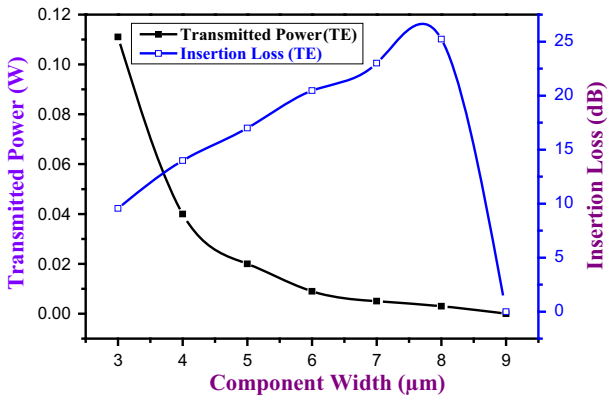


**Figure 5.** Plots between insertion loss and transmitted power vs. component width of MZI.

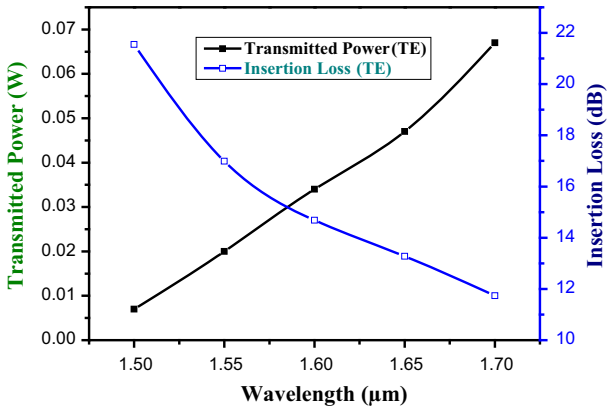


**Figure 6.** Plots between the insertion loss and transmitted power vs. wavelength of MZI.

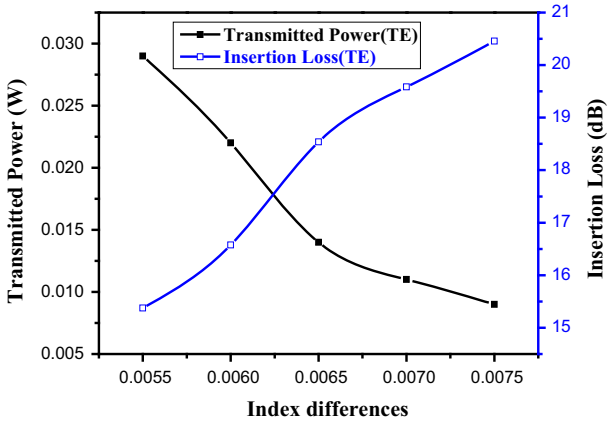


**Figure 7.** Plots between the insertion loss and transmitted power vs. index difference of MZI.

3 $\mu$m width has lesser loss (9 dB) and 8 $\mu$m width has higher loss (25 dB) on SOI-based MZI compared to InP substrate.

Operating wavelength ($\lambda$) takes an imperative role in MZI in changing the transmitted power and insertion loss. Figure 6 shows that the transmitted power and insertion loss vary with wavelength of the MZI in TE polarisation mode. The transmitted power decreases with wavelength, because the core and cladding polarisation modes possess the same wavelengths to achieve interference, which has got a lesser transmitted power of 0.06 $\mu$W at 1.7 $\mu$m wavelength. A maximum transmitted power of 0.007 $\mu$W was obtained at 1.5 $\mu$m wavelength because the effective index is proportional to the wavelength of the operating light. The insertion loss is reciprocal to the transmitted power, so that 1.5 $\mu$m wavelength has higher loss (21 dB) and 1.7 $\mu$m wavelength has lower loss (11 dB) on SOI-based MZI.

The index difference ($\Delta n$) (refractive index difference between the core material (Si) and the cladding material ($SiO_2$) with 0.3%) takes an important role in MZI for finding the transmitted power and insertion loss. Figure 7 shows that the transmitted power and insertion loss vary with index difference of the MZI in TE polarisation mode. The transmitted power is decreased with index difference, as core and cladding polarisation modes have similar wavelengths to achieve interference. Lesser transmitted power (0.009 $\mu$W) is obtained at 0.0075 index difference, while a maximum transmitted power of 0.029 $\mu$W is achieved at 0.0055 index difference. In addition, effective index is proportional to the wavelength of operating light for different paths. The insertion loss is inversely proportional to the transmitted power, so that index difference of 0.0055 has 15 dB and index difference of 0.0075 has 20 dB on SOI-based MZI which has minimum value against the $LiNbO_3$.

## 5. Conclusions

To conclude, the article proposed a novel design of phase-shifter based MZI on SOI platform and then analysed their behaviour using BPM. The desired TE-mode phase shifts were realised by changing the path lengths from 1000 to 4000 $\mu$m. 4000 $\mu$m path length has got maximum phase shift. At 1550 nm wavelength, the obtained insertion loss was 16 dB for TE mode. Similarly, at 5 $\mu$m width the insertion loss was 16 dB, 1000 $\mu$m and 4000 $\mu$m path lengths recorded an insertion loss of zero decibels and 0.0060 index differences has an insertion loss of 16 dB. This design can be used for constructing various integrated circuits such as optical modulator, LSI, demultiplexing, filtering and sensing applications because insertion loss is minimum.

## References


[1] A Liu, R Jones, L Liao, D Samara-Rubio, D Rubin, O Cohen, R Nicolaescu and M Paniccia, *Nature* **427**, 615 (2004)

[2] D Dai, Z Wang and J E Bowers, *J. Light. Technol.* **29**, 1808 (2011)

[3] F Y Gardens, G T Reed and N G Emerson, *Opt. Express* **13**, 8845 (2005)

[4] Z Han, L Liu and E Forsberg, *Opt. Commun.* **259**, 690 (2006)

[5] F Flamini *et al*, *Light Sci. Appl.* **4**, 127 (2015)

[6] H Y Choi, M J Kim and B H Lee, *Opt. Express* **15**, 5711 (2007)

[7] J Ding, H Chen, L Yang, L Zhang, R Ji, Y Tian, W Zhu, Y Lu, P Zhou, R Min and M Yu, *Opt. Express* **20**, 7081 (2012)

[8] I Goykhman, B Desiatov, S B Ezra, J Shappir and U Levy, *Opt. Express* **21**, 19518 (2013)

[9] A Agarwal, C S Kim, R Hobbs, D Van Dyck and K K Berggren, *Sci. Rep.* **7**, 1677 (2017)

[10] C Zhang, P Dulal, B J H Stadler and D C Hutchings, *Sci. Rep.* **7**, 5820 (2017)

[11] D J Thomson, F Y Gardes, J M Fedeli, Y Hu, B P P Kuo, E Myslivets, N Alic, G Z Mashanovich and G T Reed, *IEEE Photon. Technol. Lett.* **24**, 234 (2012)

[12] S H Hsu, Y Chung, C M Wang and Y C Yang, *Microw. Opt. Technol. Lett.* **56**, 2950 (2014)

[13] H Yamazaki, T Yamada, T Goh and A Kaneko, *J. Light. Technol.* **29**, 721 (2011)

[14] L B Soldano, A H de Vreede, M K Smit, B H Verbeek, E G Metaal and F H Groen, *IEEE Photon. Technol. Lett.* **6**, 402 (1994)

[15] X Zhang, J Yuan, K Wang, Z Kang, B Yan, X Sang, Q Wu, C Yu and G Farrell, *IEEE Photon. J.* **7**, 2701208 (2015)

[16] B Sepulveda, G Armelles and L M Lechuga, *Sens. Actuators A* **134**, 339 (2007)

[17] B Sepulveda, J Sanchez del Rio, M Moreno, F J Blanco, K Mayora, C Dominguez and L M Lechuga, *J. Opt. A: Pure Appl. Opt.* **8**, 561 (2006)

[18] L Li, L Xia, Z Xie and D Liu, *Opt. Express* **20**, 11109 (2012)

[19] D Perez, I Gasulla, L Crudgington, D J Thomson, A Z Khokhar, K Li, W Cao, G Z Mashanovich and J Capmany, *Nature Commun.* **8**, 636 (2017)

[20] M H Idjadi and F Aflatouni, *Nature Commun.* **8**, 1209 (2017)

[21] G F R Chen, J R Ong, T Y L Ang, S T Lim, C E Png and D T H Tan, *Sci. Rep.* **7**, 7246 (2017)

[22] Z Lu, D Celo, H Mehrvar, E Bernier and L Chrostowski, *Sci. Rep.* **7**, 12244 (2017)

[23] A Govdeli, M C Sarihan, U Karaca and S Kocaman, *Sci. Rep.* **8**, 1619 (2018)

[24] Y Chen, H Li and M Li, *Sci. Rep.* **2**, 622 (2012)

[25] A Psarouli *et al*, *Sci. Rep.* **5**, 17600 (2015)

[26] H Zhang, J Chen, J Jin, J Lin, L Zhao, Z Bi, A Huang and Z Xiao, *Sci. Rep.* **6**, 19024 (2016)

[27] H Fan and P Berini, *J. Lightw. Technol.* **31**, 2606 (2013)

[28] S W Guo and J W Wu, *J. Phys.* **87**, 91 (2016)

[29] G Zheng, L Xu and Y Liu, *Pramana – J. Phys.* **86**, 1091 (2016)

[30] www.rsoftdesign.com, BeamPROP 8.1 user guide, 14 (2008)